Global modeling of heterogeneous chemistry on mineral aerosol surfaces: Influence on tropospheric ozone chemistry and comparison to observations

S. E. Bauer,[1] Y. Balkanski, M. Schulz, and D. A. Hauglustaine

Laboratoire des Sciences du Climat et de l'Environnement, Centre National de la Recherche Scientifique/Commissariat à l'Energie Atomique, Gif-sur-Yvette, France

F. Dentener

Joint Research Center, Institute for Environment and Substainability, Ispra, Italy

Received 16 June 2003; revised 4 November 2003; accepted 10 November 2003; published 23 January 2004.

[1] Mineral aerosols can affect gas phase chemistry in the troposphere by providing reactive sites for heterogeneous reactions. We present here a global modeling study of the influence of mineral dust on the tropospheric photochemical cycle. This work is part of the Mineral Dust and Tropospheric Chemistry (MINATROC) project, which focussed on measurement campaigns, laboratory experiments, and integrative modeling. The laboratory experiments provide uptake coefficients for chemical species on mineral aerosol surfaces, which are used to compute the heterogeneous reaction rates in the model. The field measurements at Mount Cimone, northern Italy, provide trace gas and aerosol measurements during a Saharan dust episode and are used to evaluate the model. The simulations include the reactions between mineral dust aerosols and the gas-phase species O_3, HNO_3, NO_3, and N_2O_5. Under the conditions for the year 2000 the model simulates a decrease in global tropospheric ozone mass by about 5% due to the heterogeneous reactions on dust aerosols. The most important heterogeneous reaction is the uptake of HNO_3 on the dust surface, whereby the direct uptake of ozone on dust is not important in atmospheric chemistry. The comparison of the model results to observations indicates that the model simulates well the aerosol mass transported into the Mediterranean during the dust events and the arrival of all major dust events that were observed during a 7 month period. The decrease in ozone concentration during dust events is better simulated by the model when the heterogeneous reactions are included. *INDEX TERMS:* 0305 Atmospheric Composition and Structure: Aerosols and particles (0345, 4801); 0365 Atmospheric Composition and Structure: Troposphere—composition and chemistry; 0368 Atmospheric Composition and Structure: Troposphere—constituent transport and chemistry; *KEYWORDS:* heterogeneous chemistry, mineral dust, tropospheric ozone

Citation: Bauer, S. E., Y. Balkanski, M. Schulz, D. A. Hauglustaine, and F. Dentener (2004), Global modeling of heterogeneous chemistry on mineral aerosol surfaces: Influence on tropospheric ozone chemistry and comparison to observations, *J. Geophys. Res.*, *109*, D02304, doi:10.1029/2003JD003868.

1. Introduction

[2] Aerosols have an important influence on gas-phase atmospheric chemistry [*Ravishankara*, 1997; *Jacob*, 2000]. First of all, aerosols provide reactive surfaces in the atmosphere where heterogeneous chemical reactions can take place. For instance, *Dentener and Crutzen* [1993] showed the importance of heterogeneous chemistry on accumulation range aerosol for ozone and the nitrogen budget. Likewise coarse aerosols may be important for heterogeneous chemistry. In the atmosphere the coarsest particles, above >2.5 μm diameter, are mainly the natural aerosols, mineral dust and sea salt. Sea salt aerosols are predominantly present in the marine boundary layer [*Jaenicke*, 1993], while desert dust can be transported by individual storms from Africa across the Atlantic to the east coast of the United States or for example from Asia across the Pacific Ocean [*Prospero*, 1995; *Ott et al.*, 1991]. Mineral dust has been found up to a height of 8 km [*Jaenicke*, 1993]. The atmospheric residence time of mineral dust depends on the meteorological conditions and on the aerosol size. For example, large particles, with diameters of 100 μm are only found close to the source regions whereas small particles, about

[1]Now at NASA Goddard Institute for Space Studies, The Earth Institute at Columbia University, New York, New York, USA.

0148-0227/04/2003JD003868$09.00

2 μm diameter can stay in the atmosphere for several days and travel long distances.

[3] We estimate that the area of mineral aerosol surfaces is equivalent to up to 30% of the Earths surface above source regions and approximately 10% over wide parts of Africa. Furthermore the alkalinity of mineral dust favors the uptake of gaseous species and laboratory experiments have observed heterogeneous reactions taking place on dust surfaces [*Grassian*, 2001; *Hanisch and Crowley*, 2001; *Goodman et al.*, 2000; *Hanisch and Crowley*, 2003a; *Underwood et al.*, 2001; *Michel et al.*, 2002]. Mineral dust is therefore a very important aerosol, providing reactive surface in the troposphere, and a number of box, regional and global model studies have demonstrated the relevance of these heterogeneous reactions for atmospheric chemistry [*Zhang et al.*, 1994; *Dentener et al.*, 1996; *de Reus et al.*, 2000; *Phadnis and Carmichael*, 2000; *Liao et al.*, 2003; *Bian and Zender*, 2003].

[4] Another way in which aerosols influence gas phase chemical cycles is by absorbing and scattering of sun light and thus influencing the photochemical reaction rates [*Dickerson et al.*, 1997]. *He and Carmichael* [1999], *Martin et al.* [2003], and *Liao et al.* [2003] showed that the effect on ozone is small. The inclusion of aerosols in photolysis rate calculations accounts for less than 0.2 ppbv of monthly mean ozone concentration [*Liao et al.*, 2003], and *Bian and Zender* [2003] showed that the impact of mineral dust on photolysis rates leads to a global increase in predicted ozone concentrations of about 0.2% in the annual mean.

[5] Another pathway of unknown importance of aerosols influencing gas-phase chemistry could be when aerosols act as long range carriers for condensed species on their surfaces.

[6] Previous studies acknowledged reaction rates on the aerosol surfaces as the factor of highest uncertainty in their modeling work [*Dentener et al.*, 1996; *Liao et al.*, 2003]. Furthermore, there has been little experimental evidence providing the significance of heterogeneous reactions on dust. The approach of our work is to simulate the uptake of reactive gases on mineral dust surfaces in a global circulation model that includes schemes to simulate dust aerosols and atmospheric chemistry. This study is embedded in the framework of the Mineral Dust and Tropospheric Chemistry (MINATROC) project [*Balkanski et al.*, 2003a]. The project combines the molecular level details, field observations and aims to estimate the global significance of these reactions by combining laboratory investigations, measurements and atmospheric chemistry models. The laboratory studies provide mechanistic information on absorption and reaction of atmospheric gases on aerosol surfaces, and the identification of the saturating effects and product species, which are then accounted for in the model formulation. The results of the laboratory studies are incorporated into the atmospheric chemistry model in order to assess the global significance. The results of the modeling study, in turn, are compared to gas and aerosol measurements that have been observed at Mount Cimone, in northern Italy during an intensive field measurement campaign.

[7] The paper starts with a brief model description followed by the discussion of the dust simulation, in sections 2 and 3, respectively. The uptake coefficients for the single heterogeneous reactions are discussed in section 4. In section 5 the model results of the baseline and the sensitivity experiments are presented. The nitric acid cycle is discussed in section 5.3. In section 6, the model results are compared to observations, and final conclusions are drawn in section 7.

2. Model Description

[8] Laboratoire de Météorologie Dynamique, "zoom" (LMDz) is a general circulation model (GCM) developed initially for climate studies by *Sadourny and Laval* [1984]. The model has been adapted in order to simulate the transport of trace species and is coupled to the chemistry-aerosols model Interaction With Chemistry and Aerosols (INCA). The present version of the model has 19 hybrid levels from the surface to 3 hPa and a standard horizontal resolution of 2.5 degrees in latitude and 3.75 degrees in longitude. The large-scale advection of tracers is performed using the finite volume transport scheme of *van Leer* [1977] as described by *Hourdin and Armengaud* [1999]. Convective transport is simulated using the mass-flux scheme of *Tiedtke* [1989]. The planetary boundary layer scheme is based on a second-order closure approximation. The version of the chemical scheme used in this study (version CH4.1.0) describes the methane oxidation cycle including 19 photochemical reactions and 66 chemical reactions. LMDz-INCA calculates the time evolution of 33 species with a time step of 20 min. In the present version of the model, the feedback of the chemistry on the radiation is not taken into account. A zonally and monthly ozone climatology is prescribed above the tropopause based on *Li and Shine* [1995]. The interactive lightning NO_x emission used in the model is described by *Jourdain and Hauglustaine* [2001]. A detailed description and evaluation of the model is provided by *Hauglustaine et al.* [2004].

[9] Mineral dust is included in the aerosol scheme as an interactive tracer using wind speed and precipitation to calculate dust sources, transport and deposition. Tracers in the aerosol module are represented in a spectral scheme [*Schulz et al.*, 1998] and undergo gravitational settling [*Schulz et al.*, 1998], turbulent and wet deposition [*Guelle et al.*, 1998]. The source formulation is based on the mineralogy of *Claquin et al.* [1999] and is further described by *Balkanski et al.* [2003b]. The uplift of dust into the atmosphere depends on soil parameters, e.g., soil moisture, and on surface wind speed and varies as its third power. This nonlinear flux function is dependent on the model resolution. To calculate equal fluxes for different model resolutions the dust emission flux is calculated on a $1.125° \times 1.125°$ resolution and than interpolated at every time step to the current model resolution. In this way, the emission flux is comparable for all model resolutions.

[10] The model is run on its standard resolution of 96×72 grid points ($3.75° \times 2.5°$ degrees in longitude and latitude) and on a higher horizontal resolution of 160×98 ($2.25° \times 1.8°$). All simulations presented in this paper are performed at the high resolution, except the sensitivity runs discussed in section 5.2, which are run at the low resolution. The model is integrated in a nudged mode. The three dimensional wind field is relaxed toward the horizontal components of the ECMWF wind using a nudging time step of 100 minutes. Sea surface temperature and

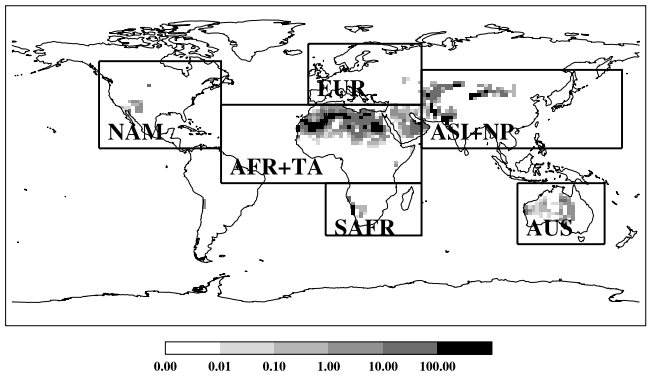

Figure 1. Annual mean soil dust emissions in g m^{-2} yr^{-1}. The six boxes classify the following regions: North America (NAM), Europe (EUR), North Africa and the tropical Atlantic (AFR + TA), South Africa (SAFR), South Asia and the eastern North Pacific (ASI + NP), and Australia (AUS).

10 m wind fields are prescribed taken from ECMWF analysis data sets on a 6 hour time step. All simulations are run for the conditions of the year 2000, after a spin-up time of one year.

3. Dust Simulation

[11] The major areas of desert dust mobilization are the Sahara and the Sahel regions, in North Africa, the Rub-al-Khali, Kara-Kum, Kyzil-Kum and Thar deserts, stretching from the Arabian Peninsula to India, and the Taklamakan and Gobi desert in China. Smaller dust mobilization events takes place in southern Australia, Namibia, Chile, Mexico and in the western United States. The map of the simulated annual mean dust emission flux for the year 2000 is presented in Figure 1. Our total annual dust emission is 905 Tg yr^{-1}. The range of source strengths found in Literature is very wide, ranging from 200 to 5000 Tg yr^{-1} [*Goudie*, 1983]. Recent model studies estimate yearly emission fluxes between 800 and 1500 Tg yr^{-1} [*Tegen and Miller*, 1998; *Tegen et al.*, 2002; *Woodward*, 2001; *Zender et al.*, 2003; *Lunt and Valdes*, 2002].

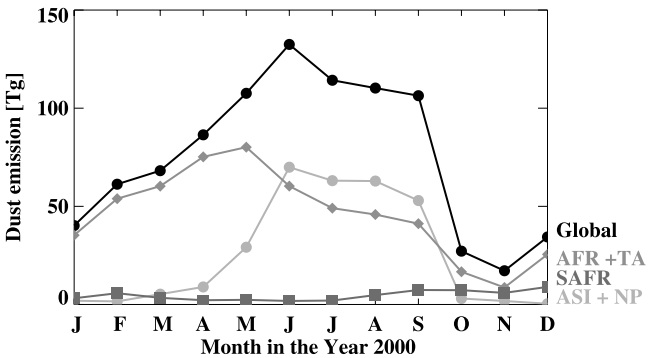

Figure 2. Time series of soil dust emissions Tg $month^{-1}$ for the global total (black line) and the contributions from the regions as indicated in Figure 1: AFR + TA (gray line with diamonds), ASI + NP (gray line with circles), and SAFR (gray line with squares).

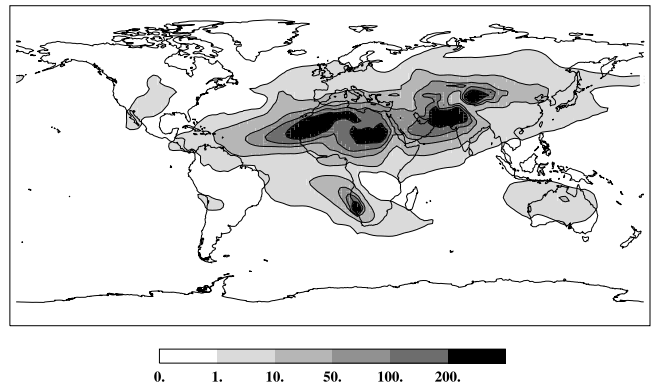

Figure 3. Annual mean total dust load (mg m^{-2}).

[12] In this paper we investigate the influence of heterogeneous chemistry in different regions. The single regions are indicated in Figure 1 and will be named by their acronyms hereafter: North America (NAM), Europe (EUR), North Africa and the tropical Atlantic (AFR + TA), South Africa (SAFR), south Asia and the eastern North Pacific (ASI + NP), and Australia (AUS). The time series of our monthly mean dust emission fluxes (Figure 2) shows global sources reaching maximum intensity during the Northern Hemispheric summer. The regional contributions to this global cycle (Figure 2) indicate that the North African (ARF + TA) dust sources dominate the global emission sources and show maximum dust uplifts during spring. The dust fluxes in the (ASI + NP) region shows maximize fluxes in June and July. The other regions show only minor contributions to the global dust flux budget.

[13] Figure 3 shows the horizontal distribution of the annual load of mineral dust. The North African dust cloud covers the whole North African continent, travels over the tropical Atlantic and dust loads of about 10 mg m^{-2} are found over the coast of the South American continent. High dust loads are predicted over Pakistan, India and east China and downwind of those regions. Altogether a band of high dust loads (above 50 mg m^{-2}) is formed, stretching from 30°W to 120°E in the Northern Hemisphere lower latitudes. In the Southern Hemisphere, the South African dust source shows a significant contribution followed by the Australian dust. Further dust clouds are simulated in North America and Chile.

[14] Evaluation of mineral aerosol simulations are very difficult. Our model is best evaluated for Saharan dust. *Schulz et al.* [1998] tested the dust model against satellite retrievals in the Saharan regions and found a good agreement for the simulated dust optical thickness and the aerosol size distribution. Later in this paper, chapter 6.2 and 6.3 we show a comparison to in situ measurements and the model demonstrate a remarkable simulation of dust in the Mediterranean (see Figure 14). Compared to satellite retrievals [*Herman et al.*, 1997; *Husar et al.*, 1997], POLDER (http://smsc.cnes.fr/POLDER) and TOMS satellite maps (http://toms.gsfc.nasa.gov) for the year 2000, we find that the outflow of Saharan dust over the Atlantic ocean is very well simulated, but the outflow of dust from Asia over the North Pacific seems to be strongly underestimated by the model. Especially the well-observed springtime maximum [*Prospero et al.*, 2002] is missing in our simulation. The

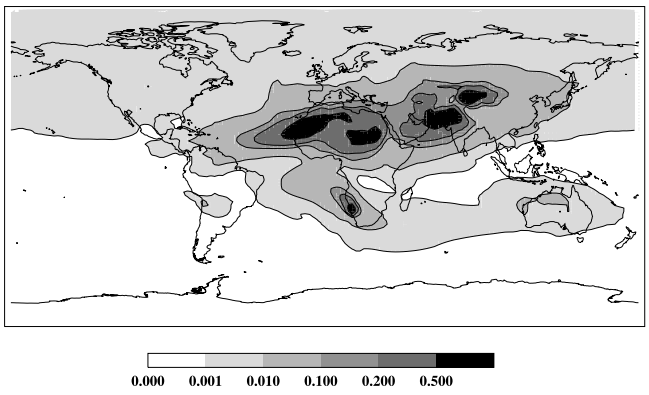

Figure 4. Annual mean dust surface per Earth surface (m^2 m^{-2}).

reason for the underestimation in Asia is probably missing dust sources in Asia in the source strength map used in the model dust source formulation. One further explanation for the underestimated dust uplift are too large precipitation rates and soil moisture in the circulation model over China, which inhibits dust uplift in our source formulation. Further comparison to the satellite retrievals show that the high optical thicknesses in the summer over the Indian ocean are consistent with the high dust burden simulated by the model, and the background concentrations of about $\leq$0.1 mg m^{-2} over the oceans in higher latitudes are reasonable simulated as well.

[15] Compared to other model simulations [*Tegen and Miller*, 1998; *Tegen et al.*, 2002; *Woodward*, 2001; *Zender et al.*, 2003] we calculate rather low dust loads. Therefore it is not likely that we overestimate the available mineral dust surface area in the atmosphere. However, the aerosol surface area depends on the aerosol size distribution. Large particles settle out very quickly and small particles can travel large distances. The dust aerosol surface area is shown in Figure 4. Dust surfaces of 0.1 m^2 m^{-2} are present over the wide Northern Hemispheric dust plume and peak surfaces above 0.5 m^2 m^{-2} over the dust source regions. In the industrialized regions, dust aerosol provide reactive surfaces of 0.005 m^2 m^{-2} in the western United States and up to 0.03 m^2 m^{-2} in southern Europe. Vertically, mineral dust is mainly present between 500 m and 5 km altitude. Compared to the simulation by *Dentener et al.* [1996] mineral dust aerosol surfaces are greater over the tropical Atlantic and less over Australia and North America, but the overall distributions are very similar, which facilitates comparison to the results obtained in that study.

4. Uptake of Gases on Mineral Dust

[16] Several atmospheric trace gases are known to react on the surface of mineral dust aerosol. The importance of single reactions for atmospheric chemistry depends on the rates of these heterogeneous reactions compared to the gas-phase loss rates. The timescales of the species specific heterogeneous reactions are described by the uptake coefficient, γ.

4.1. HNO_3

[17] The reaction of nitric acid with mineral dust aerosols has been recently addressed by several laboratory studies [*Hanisch and Crowley*, 2001; *Goodman et al.*, 2000; *Hanisch and Crowley*, 2003b; *Underwood et al.*, 2001]. This reaction irreversibly removes HNO_3 from the gas phase. *Hanisch and Crowley* [2001] have studied the uptake of HNO_3 on various mineral dust surfaces with a Knudsen reactor and propose uptake coefficients in the range between 0.08 and 0.2 for a range of dust samples and recommend a steady state $\gamma_{HNO_3} = 0.1$ to be used in atmospheric modeling studies. No dependence of the uptake coefficient on the $CaCO_3$ content in the dust sample was observed *Hanisch and Crowley* [2003b]. The authors did not observe gas phase nitrogen containing products on timescales similar to the uptake and thus confirm the assumption of an irreversible uptake. Furthermore they found the uptake to be independent of humidity. *Goodman et al.* [2000] and *Underwood et al.* [2001] propose a smaller uptake coefficient of $\gamma_{HNO_3} = 2.5 \pm 0.1 \times 10^{-4}$ under dry conditions, which increases in the presence of water vapor. *Goodman et al.* [2000] discuss their measured γ_{HNO_3} to represent an initial coefficient for the uptake of HNO_3 on $CaCO_3$ particles near 0% RH, representing a lower limit to the true uptake coefficients which they assume probably to be closer to $\gamma_{HNO_3} = 2.5 \times 10^{-3}$ or even greater. They also conclude the uptake of HNO_3 to be irreversible. In the present modeling study we rely on the uptake coefficient of *Hanisch and Crowley* [2001] ($\gamma_{HNO_3} = 0.1$) for our standard simulation, which has been confirmed by measurements conducted by the same group but using a aerosol flow reactor (MINATROC, unpublished project report, 2003). However, to take into account the range of uncertainty found in literature we perform sensitivity studies were γ_{HNO_3} of 0.25, 0.05 and 0.001 will be tested.

4.2. O_3

[18] The uptake coefficient of ozone on mineral aerosols is much better agreed in literature. *Michel et al.* [2002, 2003] measured uptake coefficients ranging between $\gamma = 1 \times 10^{-5}$ and 7×10^{-6} for various mineral oxide powders. *Hanisch and Crowley* [2003a] have measured the uptake of O_3 on Saharan dust and determine a steady state $\gamma = 7 \times 10^{-6}$ at tropospheric O_3 concentrations (30 ppb_v), with an initial uptake coefficient $\gamma_0 = 3 \times 10^{-5}$. Ozone is destroyed on the mineral aerosol surface and O_2 is produced. Furthermore they found that the aerosol surface could be completely neutralized by the extended presence of elevated O_3 concentrations. For this modeling study we select $\gamma_{O_3} = 1 \times 10^{-5}$ and we do not account for possible surface deactivation processes. In the sensitivity experiments we test $\gamma_{O_3} = 3 \times 10^{-5}$ and 3×10^{-6} as upper and lower limit. Taking into account that the uptake of ozone on mineral dust depends on the ambient ozone concentration, the lower limit γ_{O_3} seems to be more appropriate for global modeling.

4.3. N_2O_5

[19] Nighttime hydrolysis of N_2O_5 on several aerosol and aqueous surfaces is a major atmospheric sink of NO_x [*Dentener and Crutzen*, 1993]. The uptake of N_2O_5 on aerosol surfaces depends on humidity, whereby the uptake probability increases with increasing humidity [*Hu and Abbatt*, 1997]. For mineral dust an uptake coefficient ranging between $\gamma_{N_2O_5} = 0.02$ (rH = 70%) and 0.003 (rH = 30%) is used in our model simulation based on

recommendations by J. Crowley (personal communication, 2003). These values are lower than $\gamma_{N_2O_5} = 0.05$ used in prior model studies [e.g., *de Reus et al.*, 2000; *Dentener et al.*, 1996].

4.4. NO_3

[20] Not much is known about the uptake of NO_3 on mineral dust surfaces. It is assumed that particulate nitrate is formed irreversibly by the mass transfer of NO_3 on the aerosol surface. In this study we use a low uptake coefficient of $\gamma_{NO_3} = 3 \times 10^{-3}$. This value lies in between the measurements of γ_{NO_3} on salt solutions [*Thomas et al.*, 1998] $\gamma_{NO_3} > 2 \times 10^{-3}$, and water and different ionic solutions [*Rudich et al.*, 1996] $\gamma_{NO_3} = 0.15 - 6 \times 10^{-3}$ and was also used in prior model simulations [*de Reus et al.*, 2000].

[21] Although, other gaseous species can undergo heterogeneous reactions on the surface of mineral aerosols. The uptake of NO_2 may lead to surface products of nitrate and nitrite on the aerosols, but the reaction is very uncertain, and probably for global photooxidant levels this process is of minor importance. Hydroxyl and HO_2 radicals also react on aerosol surfaces. The OH heterogeneous removal rates are very slow compared to gas phase production and destruction rates and is therefore negligible [*Bian and Zender*, 2003]. Uptake of HO_2 on aerosols might have an impact on atmospheric chemistry [*Saylor*, 1997], but laboratory measurements are needed to investigate this reaction. *Martin et al.* [2003] concluded in their modeling study, that the uptake of HO_2 by aerosols are of importance over polluted regions, with large amounts of sulfate and organic carbon, and over biomass burning areas, with high concentrations of organic carbon. *Grassian* [2001] studied the uptake of volatile organic compounds and found acetaldehyde, acetone and propionaldehyde to be sensitive to heterogeneous reactions on mineral dust particles. This process could be of importance for secondary aerosol formation. Heterogeneous reaction of SO_2 on dust is potentially a very important uptake process [*Dentener et al.*, 1996]. This reaction pathway is neglected in our study because we focus on the influence of heterogeneous reactions on ozone chemistry.

[22] The following effective reaction pathways are considered in the present model study:

$$HNO_3(\text{gas}) \rightarrow NO_3^-(\text{aerosol}), \quad (1)$$

$$N_2O_5(\text{gas}) \rightarrow 2NO_3^-(\text{aerosol}), \quad (2)$$

$$NO_3(\text{gas}) \rightarrow NO_3^-(\text{aerosol}), \quad (3)$$

$$O_3(\text{gas}) \rightarrow 3O_2. \quad (4)$$

4.5. Formulation of Heterogeneous Uptake in the Model

[23] In the model formulation the uptake of gases on aerosol surfaces is described by a pseudo first-order rate coefficient k_j (s^{-1}) which gives the net removal rate of gas-phase species j to an aerosol surface:

$$k_j = \int_{r^2}^{r^1} k_{d,j}(r) n(r) dr, \quad (5)$$

Table 1. Uptake Coefficients as Used for the Simulations (Best Guess) and Sensitivity Experiments (Upper and Lower Limit)[a]

	Best Guess	Upper Limit	Lower Limit	Special
HNO_3	0.1	0.25	0.05	0.001
NO_3	0.003			
N_2O_5	f(rH)	0.05	0.003	
O_3	1×10^{-5}	3×10^{-5}	3×10^{-6}	

[a]The uptake coefficient of N_2O_5 is dependent on relative humidity and ranges linearly between $\gamma_{N_2O_5} = 0.02$ (rH = 70%) and 0.003 (rH = 30%).

with $n(r)dr$ (m^{-3}) is the number density of particles between the aerosol radius interval r and $r + dr$. $k_{d,j}$ describes the size-dependent mass transfer coefficient ($m^3\ s^{-1}$) calculated using the *Fuchs and Sutugin* [1970] equation:

$$k_{d,j} = \frac{4\pi D_j V}{1 + K_n\left(\lambda + 4\frac{(1-\gamma_j)}{3\gamma_j}\right)}, \quad (6)$$

where D_j is the gas-phase molecular diffusion coefficient of a trace gas in air ($m^2\ s^{-1}$):

$$D_j = \frac{3}{8Ad_q^2\rho_a}\sqrt{\frac{R^\star T m_a}{2\pi}\left(\frac{m_q + m_a}{m_q}\right)} \quad (7)$$

[e.g., *Chapman and Cowling*, 1970; *Davis*, 1983], where A is Avogadro's number, ρ_a density of air, $R^\star$ gas constant, T is the temperature, m_a, m_q molecular weight of air and gas q, d_q is the diameter of the gas molecule ($\approx$4.5 $\AA$). Further variables used in equation (6) are, the ventilation coefficient V (set to unity in our experiments), K_n the Knudsen number, λ is the effective free pathway of a molecule in air, and γ_j, the uptake coefficients of a gas on aerosol surfaces as determined by the laboratory studies. The values for γ_j that are used in our model study are summarized in Table 1.

[24] Figure 5 shows the annual and zonal mean distribution of the reaction rate for nitric acid, k_{HNO_3}. According to the distribution of the dust surface area the reaction rate has high values in the lower latitudes of the Northern Hemisphere.

5. Model Results

5.1. Influence of the Uptake on Ozone Concentrations

[25] This section presents how ozone concentrations are affected by the heterogeneous uptake of gases. The model results will be discussed by comparing control simulations, where no interaction between mineral aerosols and gas phase species take place (hereinafter CTR), to a simulation with heterogeneous chemistry (hereinafter HET). In the HET simulation, the uptake of HNO_3, N_2O_5 NO_3 and O_3 on dust is included using the best guess values for the uptake coefficients as described in the previous chapter. The CTR and the HET simulations use the high model resolution (2.25° × 1.8°) and are run for the conditions of the year 2000.

[26] The changes in the ozone concentration fields are discussed in Figure 6. The annual near-surface ozone concentration field (Figure 6, upper left panel) is characterized by high ozone concentrations over the industrialized regions of North America and Europe, extending to the

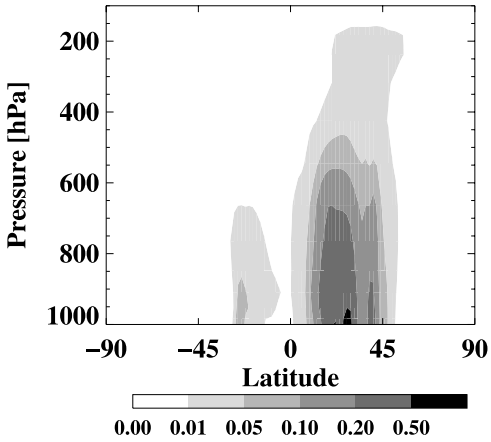

Figure 5. Zonal and annual mean reaction rate for the uptake of HNO_3 on dust ($\times 10^3$ s^{-1}).

Middle East. High ozone concentrations are also found in regions of biomass burning over Brazil and equatorial Africa. The high ozone concentrations in the mountain regions such as the Himalaya, Greenland and the Rocky Mountains correspond to ozone from higher altitudes. Heterogeneous reactions on dust reduce ozone (Figure 6, middle left panel) with maximum reduction at surface levels, of about 5–10 ppb_v, over the North African continent, the Arabian Peninsula and the Middle East. Furthermore, a narrow band of reduced surface ozone mixing ratios is spanning over the southern tropical Atlantic. Surface ozone is reduced by more than 1 ppb_v in the whole Northern Hemisphere. In percentage terms (Figure 6, lower left panel), the destruction amounts to 20% of ozone in the tropical region and even 2–5% in regions devoid of any significant dust amounts.

[27] At higher altitudes, at 500 hPa, ozone concentrations are distributed more zonally with a strong gradient between the two Hemispheres, as shown for the CTR simulation in Figure 6, upper right panel. Maximum Northern Hemispheric ozone concentrations are simulated over the Middle East and a weak ozone maximum is seen in the tropical convergence region over Africa, where ozone is transported upward by biomass burning and the tropical convective system. Heterogeneous reactions on dust influence ozone most strongly in the equatorial region reaching from west Africa to India with changes of up to 10 ppb_v, which represents 10% of the ozone burden in these regions (Figure 6, middle and lower right panel). Locally, in the center of this region ozone is reduced by up to 20%.

[28] To better understand the changes in ozone, the changes in the NO_y concentration fields needs to be analyzed. The most significant change in a nitrogen containing species is seen in the nitric acid concentration field. Figure 7 shows the distribution and changes of near-surface nitric acid concentrations. Maximum nitric acid concentrations occur close to the surface over the heavy industrialized regions and in the tropical areas of biomass burning. Nitric acid destruction by heterogeneous reactions on dust removes over 50% of surface HNO_3 over a wide region, covering the tropical Atlantic, Africa and east Asia. The changes in the concentration field (Figure 7, middle panel) shows that about 1 ppb_v of nitric acid is removed in the biomass burning areas. In contrast, HNO_3 concentrations in industrial areas are more or less unaffected. However, the main decreases in the near-surface ozone concentrations, occur close and downwind of the areas of maximum HNO_3 destruction. This strong impact of HNO_3 removal on ozone can be explained by the role of HNO_3 as a reservoir species. Nitric acid uptake on dust prevent it's renoxification by photolysis and reaction with OH. Nitrogen oxides are mainly released in urban and regional areas and have a too short life time to influence background ozone chemistry. NO_x reservoir species, therefore determine ozone concentrations in the clean atmosphere, and so, the loss of precursor species in remote regions, through surface reactions on mineral dust, has such a strong influence on the global ozone budget.

[29] Table 2 summarizes concentration changes in percentage relative to the tropospheric mass of the gaseous species. We assume the first ten model layers (which represent approximately the 200 hPa pressure level) to represent the troposphere in the model. Globally, the loss of the four species under study are: HNO_3 (35%), N_2O_5 (11%), NO_3 (18%), and O_3 (5%). These are the species that are directly reacting with the aerosols. Changes to OH are quite significant with a global decrease of 7%, and 13% over Africa, indicating a change of oxidation capacity due to the introduction of this additional heterogeneous reaction pathway.

[30] The general results presented in this chapter depend on a variety of assumptions drawn for this specific simulation. The robustness of these results are tested in a set of sensitivity experiments focussing on the uncertainty of the single uptake coefficients, the importance of the single heterogeneous reactions (equations (1)–(4)), and the dust load.

5.2. Sensitivity Experiments

5.2.1. Importance of the Single Reactions

[31] In this sensitivity study the model was integrated each time for the period of 12 months, at the lower model resolution (3.75° × 2.5°). In each simulation only one species was allowed to react on the surface of the mineral dust. The results of this set of sensitivity experiments are discussed in Figure 8 and Table 3, where the percentage loss in ozone relative to the tropospheric mass of ozone is shown. The black circle on the left in Figure 8 shows the result of the previous discussed simulation (uptake of all four gases, but now simulated on the low model resolution) and the four following circles give the results of the four sensitivity runs (single gas uptake only). Globally, 5.4% of the tropospheric ozone mass is removed by reactions between the four gases and the aerosol surfaces. (For the global budget we retrieve the same percent changes as calculated on the high model resolution, see Table 2). In the sensitivity run, where only HNO_3 was allowed to react on the aerosol, a reduction of 4.4% in ozone mass was calculated. The single uptakes of N_2O_5, NO_3 or O_3 have a much smaller influence on the ozone concentrations, ozone is reduced globally by 0.7, 0.4 and 0.5%, respectively. Regionally the strongest impact is seen in the African region, but the relative importance of the uptake of the single species does not depend on the region. The uptake of nitric acid clearly dominates the other heterogeneous reac-

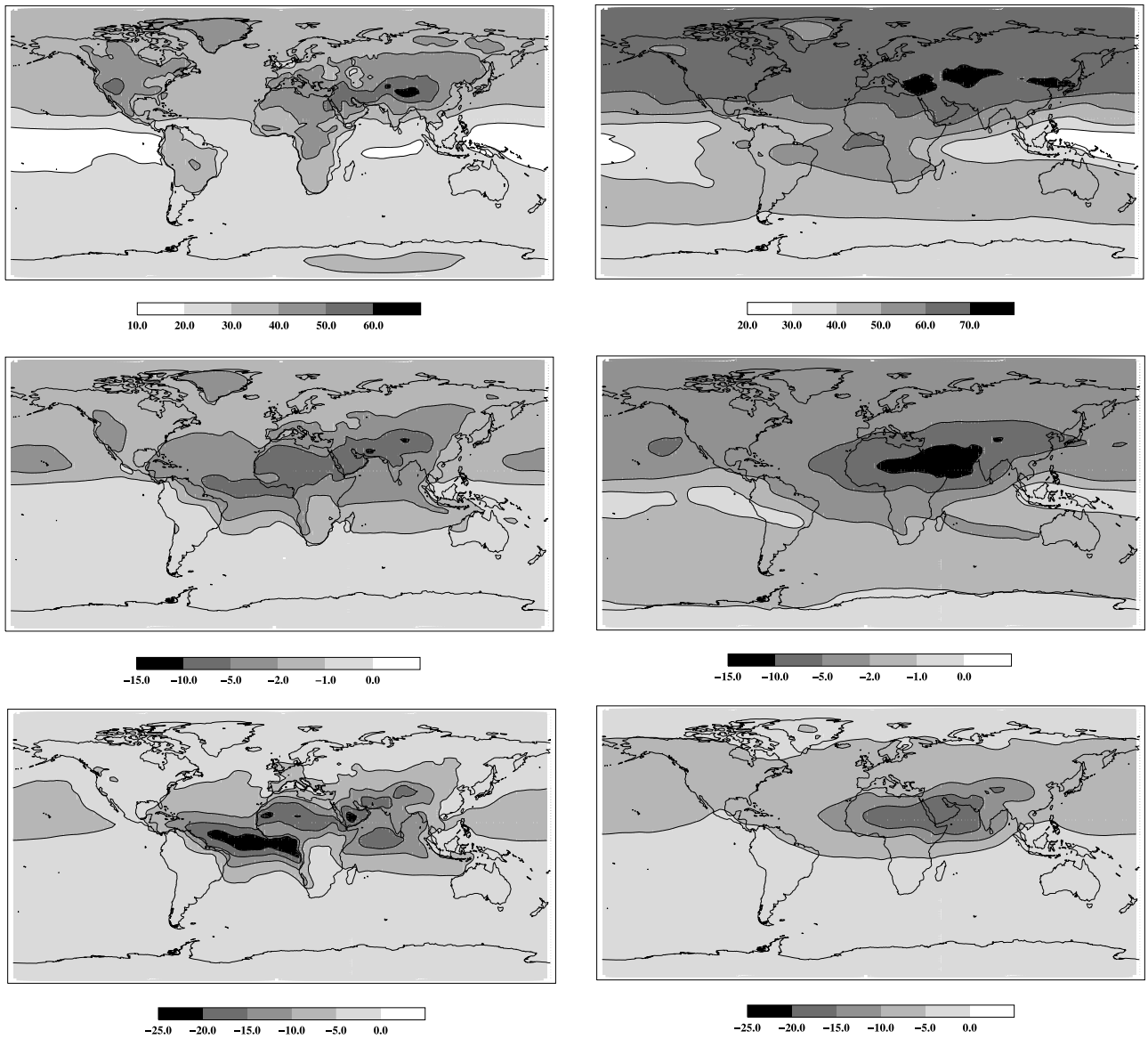

Figure 6. Annual mean ozone concentrations close to the surface, i.e., in the (top left) first model layer and in (top right) 500 hPa height in the control simulation. The middle and bottom panels show the differences due to heterogeneous chemistry (HET − CTR) relative to this control simulation in (middle) units of volume mixing ratios (ppb_v) and (bottom) percentage changes (100 × (HET − CTR)/CTR), respectively, for the near-surface (left panel) and the 500 hPa (right panel) height level.

tions. This in turn shows that our prediction of the effect of mineral aerosols on the ozone budget depends very much on the quality of the simulated nitric acid concentration field. To take that point into account we compare the nitric acid concentrations to observations (section 6) and discuss the simulated nitric acid budget in section 5.3.

5.2.2. Uncertainty of the Uptake Coefficients

[32] A further uncertainties when studying the influence of heterogeneous processes on atmospheric chemistry relates to the uptake coefficients. These coefficients were the most uncertain factors in previous studies [*Dentener et al.*, 1996; *de Reus et al.*, 2000; *Liao et al.*, 2003]. We therefore performed additional sensitivity studies where we varied the uptake coefficients but only tested the single reactions. The uptake coefficients listed as upper and lower limits in Table 1 were used for this sensitivity test. The corresponding results are shown in Figure 8, were the upward triangles refer to upper limit and the downward triangles reflect the lower limit uptake coefficients.

[33] The uptake coefficient of O_3 was varied by the factor three around the best guess value, thus γ_{O_3} between 3×10^{-5} and 3×10^{-6}. This values cover the factor of uncertainty reported by *Hanisch and Crowley* [2003a]. The simulation shows that the ozone concentrations are not very sensitive to the direct uptake of ozone on dust alone and to the variation of γ_{O_3}. When the high γ_{O_3} is used, 0.7% of tropospheric ozone mass is depleted just by the direct uptake of ozone molecules on the aerosols. However when γ_{O_3} lies between our "best guess" and the "lower limit" value the impact on the global ozone mass of this heterogeneous reaction is very small. *Hanisch and Crowley* [2003a] suggest $\gamma_{O_3} = 7 \times 10^{-6}$ to be used in atmospheric

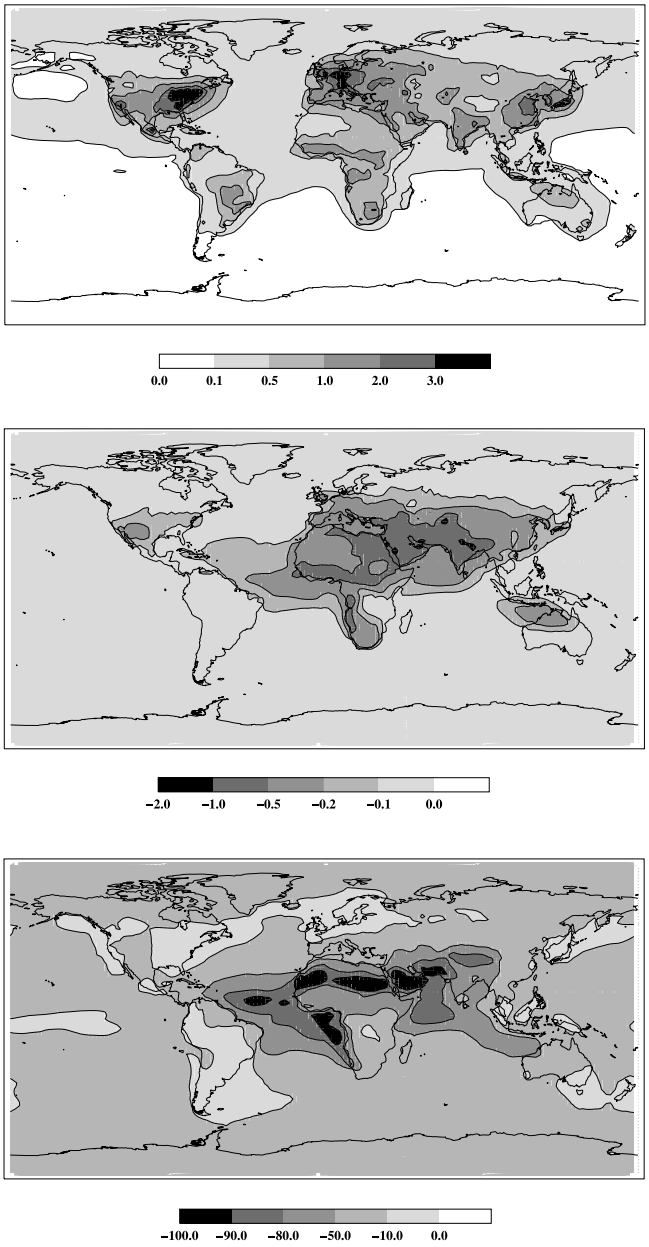

Figure 7. (top) Annual mean near-surface nitric acid concentration of the CTR run in ppb_v. Changes (HET – CTR) in near-surface nitric acid concentration in (middle) ppb_v and (bottom) percentage.

modeling, which corresponds to a value between our "best guess" and the "lower limit". We conclude that the direct uptake of ozone might only be of importance in limited areas of very high dust concentrations, but it is not important for global atmospheric chemistry.

[34] The uptake of N_2O_5 on mineral dust depends on humidity (see chap. 4). In the sensitivity test we used the $\gamma_{N_2O_5}$, given for dry and humid conditions as upper and lower limit, respectively. The results show that when testing the high uptake coefficient, 0.8% of the global ozone mass is removed by the uptake of N_2O_5 on aerosols and when the lower limit of $\gamma_{N_2O_5}$ is tested, the reaction has no impact on the ozone budget. When $\gamma_{N_2O_5}$ is calculated as a function of humidity it happens to be the second most important heterogeneous reaction responsible for tropospheric ozone destruction.

[35] The uptake of HNO_3 is the most important reaction in this study and the true range of the uptake coefficients is still under discussion. Our study is based on the work of *Hanisch and Crowley* [2001, 2003b] favoring a best guess $\gamma_{HNO_3} = 0.1$, based upon Knudsen cell experiments on different dust-like and real dust substrates. In the sensitivity study the uptake coefficient for HNO_3 is varied between 0.05 and 0.25. No differences in ozone loss are seen in the results of the simulations when γ_{HNO_3} is changed. Thus the uptake coefficient is already so high that this reaction is not limited by the sticking probability, which means that HNO_3 reacts very efficiently on the surfaces of mineral aerosols. A further sensitivity test is performed using $\gamma_{HNO_3} = 0.001$ proposed by *Goodman et al.* [2000] and *Underwood et al.* [2001] and used in the modeling work of *Bian and Zender* [2003]. Lowering the uptake coefficient of HNO_3 by two orders of magnitude leads to half of the impact on the ozone concentrations (see gray diamond 1 in Figure 8). We simulated 2.2% decrease in ozone. *Bian and Zender* [2003] simulate 0.9% including several heterogeneous reactions. These differences can be caused by several differences in the model formulations: For example, differences in the dust surface areas, chemistry schemes, and trace gas concentrations, or differences in computing the heterogeneous removal rates. Figure 9 shows the horizontal distributions of ozone and nitric acid decreases for this sensitivity experiment, $\gamma_{HNO_3} = 0.001$, and can be compared to the results of the baseline experiment in Figures 6 and 7. The general pattern remain unchanged but with an reduced amplitude. For example the strongest ozone reduction is still seen over the tropical Atlantic but ozone is only

Table 2. Percentage Difference in Species Concentrations (HET-CRT) in the Troposphere (Model Layer 1–10) Due to the Uptake of All Gases on the Dust Surface

	ΔO_3	ΔHNO_3	ΔNO_2	ΔN_2O_5	ΔNO_3	ΔOH
Global	−5.4	−35.3	−1.4	−10.6	−17.7	−6.6
Northern Hemisphere	−6.8	−38.0	−1.1	−12.9	−22.9	−8.2
Southern Hemisphere	−3.5	−25.5	−2.5	−5.3	−7.2	−4.4
Africa + TP	−12.2	−66.9	−9.4	−22.9	−29.8	−12.9
Asia + NP	−7.6	−48.5	−3.0	−19.7	−25.9	−8.5
Australia	−3.1	−26.5	−1.8	−4.8	−5.8	−3.4
Europe	−3.5	−15.5	+2.2	−2.1	−2.9	−2.3
North America	−4.4	−11.8	+1.6	−3.6	−4.3	−3.8
South Africa	−4.3	−41.2	−3.7	−10.2	−13.7	−5.0

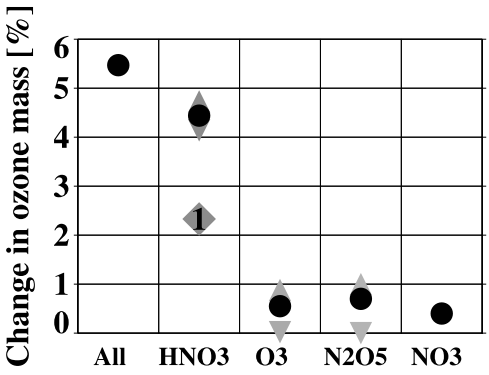

Figure 8. Percentage changes in ozone mass (CTR − HET). Black circles show the results when using the best guess uptake coefficient, and the gray triangles show the results when testing the upper (upward triangle) and lower (downward triangle) limits of the coefficients (see Table 1). The gray diamond shows the result for $\gamma_{HNO_3} = 0.001$.

reduced by 10% in its maximum instead of 25% as simulated in the baseline experiment.

[36] The overall result of these sensitivity tests is that the quality of the HNO_3 concentration field and the chosen uptake coefficient for HNO_3 is of great importance, because of the very strong impact of the heterogeneous removal of nitric acid on the ozone budget. The modeled nitric acid concentrations will be further discussed in chapter 5.3 and compared to observations in chapter 6.

5.2.3. Impact of Different Dust Loads

[37] This paper focuses on the year 2000. All conclusions are drawn following the conditions and the simulated dust load of that year, 905 Tg yr^{-1}. To study the sensitivity of our findings depending on the dust load we performed three additional experiments where the threshold velocity in the dust source formulation was modified leading to dust loads of 300, 680 and 1200 Tg yr^{-1}. The impact on the tropospheric ozone concentrations increases with increasing dust loads (Figure 10). The increase is linear up to the dust load of the year 2000, e.g., 905 Tg yr^{-1}. Further increase of dust aerosol loading then lead only to a smaller increase of the effect on tropospheric ozone. This experiment can be interpreted as the possible year to year variability in the investigated effect, that we can expect when the model would be integrated for a longer time period.

5.3. Nitric Acid

[38] The following reactions are included in the LMDz-INCA model for the representation of the nitric acid cycle. Nitric acid is produced by the reaction of NO_2 and OH, reactions with NO_3 and by hydrolysis of N_2O_5 on aerosol surfaces:

$$NO_2 + OH + M \rightarrow HNO_3 + M, \quad (8)$$

$$NO_3 + HO_2 \rightarrow 0.4HNO_3 + 0.6OH + 0.6NO_2, \quad (9)$$

$$CH_3O + NO_3 \rightarrow CO + HO_2 + HNO_3 \quad (10)$$

and the heterogeneous reactions:

$$N_2O_5 \rightarrow 2HNO_3, \quad (11)$$

$$NO_3 \rightarrow HNO_3 + OH, \quad (12)$$

$$NO_2 \rightarrow 0.5HNO_3 + 0.5HNO_2. \quad (13)$$

Nitric acid is renoxified by the following reactions:

$$HNO_3 + OH \rightarrow H_2O + NO_3 \quad (14)$$

$$HNO_3 + h\nu \rightarrow OH + NO_2 \quad (15)$$

and is removed by dry and wet deposition and deposition on mineral aerosol surfaces.

[39] The simulated annual budget of nitric acid is presented in Table 4. The budgets are given for the CTR and the HET simulation. The most important source of HNO_3 is NO_2, followed by the hydrolysis of N_2O_5. NO_3 provides only a very small source for HNO_3. The annual HNO_3 production decreases on average by about 10% in the HET compared to the CTR simulation. Dry and wet deposition are the dominant sinks for HNO_3 and are of comparable importance. The uptake on dust aerosols is the third most important process. Comparing the total annual burden of nitric acid in the two simulations, HNO_3 is reduced by 35% from 3.2 to 2.1 Tg yr^{-1}.

[40] In our model simulation nonmethane hydrocarbon chemistry (NMHC) is neglected, including the formation of PAN and other organic nitrates. These simplifications can impact the results presented in this paper, because it is known that NMHC have an impact on the NO_x content in the atmosphere. *Houweling et al.* [1998] summarized from

Table 3. Percentage Difference in Ozone Concentrations Due to the Uptake of All Gases on the Dust Surface and the Uptake of the Single Gases HNO_3, O_3, N_2O_5, and NO_3, Respectively

	All	HNO_3	O_3	N_2O_5	NO_3
Global	−5.4	−4.4	−0.5	−0.7	−0.4
Northern Hemisphere	−6.8	−5.2	−0.9	−1.1	−0.7
Southern Hemisphere	−3.5	−3.2	−0.1	−0.1	−0.1
Africa + TP	−12.2	−9.0	−1.6	−1.3	−0.7
Asia + NP	−7.6	−5.6	−1.1	−1.1	−0.4
Australia	−3.1	−2.9	0.0	−0.1	0.0
Europe	−3.5	−2.9	−0.3	−0.5	−0.8
North America	−4.4	−3.8	−0.3	−0.6	−0.4
South Africa	−4.3	−3.7	−0.2	0.0	0.1

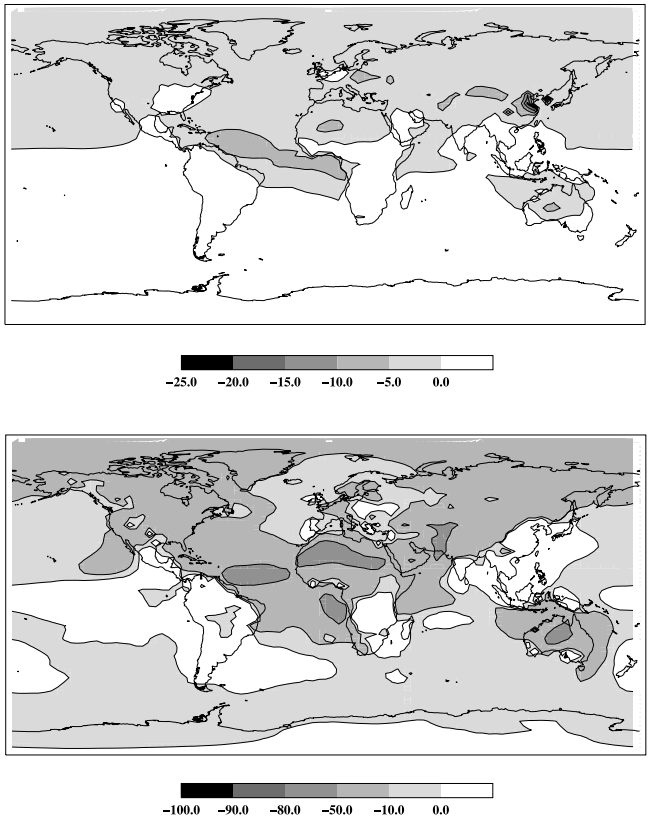

Figure 9. Difference in (top) annual mean ozone and (bottom) nitric acid concentration close to the surface due to heterogeneous chemistry relative to the control simulation in percentage changes (100 × (HET − CTR)/CTR). The HET experiment considers the uptake of HNO_3 only, with $\gamma_{HNO_3} = 0.001$.

there global modeling work, that NMHCs are important over polluted regions and that PAN production reduces the available NO_x concentrations, which in term will lead to reduced HNO_3 concentrations. *Jacob et al.* [1996] analyzed aircraft measurements over the South Atlantic and concluded that PAN thermolysis is the most important pathway of NO_x production in the lower troposphere at that specific location.

[41] The coupled aerosol-chemistry simulations presented in this paper are limited to the CH_4 chemistry scheme, but to estimate the effect that might be caused by higher chemistry on our experiment we performed a simple experiment with the Chemical Transport Model TM3, including NMHC chemistry (the same model was used in the above mentioned study by *Houweling et al.* [1998]). An ordinary NMHC chemistry run will be compared to an experiment where the thermal decomposition of PAN is neglected. Figure 11 shows the differences of those two experiments for the month of July, where the influence of PAN chemistry on HNO_3 concentrations is strongest. Neglecting PAN leads to an increase of HNO_3 in the high NO_x regions and to an decrease of up to 25% over the oceans. In the most prominent dust regions, for example North Africa and the Atlantic ocean, HNO_3 decreases by about 10%. We performed a series of box model studies (at the boxes indicated in Figure 11, at 4 km height) using a CH_4 chemistry versus a NMHC chemistry scheme including and excluding heterogeneous reactions on dust surfaces. At all three locations the simulated ozone amounts barely differ (less than 0.3%) when using the different chemistry schemes. The heterogeneous reaction rates are so fast in the presence of dust, that HNO_3 is removed very efficiently. This result is not affected by the complexity of the chemistry scheme. However, the box model simulation was representative of atmospheric conditions at 4 km height, and so this does not preclude a greater impact of PAN chemistry at higher altitudes. Furthermore, in the real atmosphere mixing process play a very important role, and these are not taken into account in a box model simulation. Nevertheless, a more complex gas-phase chemistry scheme might decrease the effect of heterogeneous dust reactions on ozone chemistry on the global scale.

[42] Furthermore, we neglect possible removal pathways on other aerosol surfaces. For example, sea salt aerosols react with HNO_3 in the marine boundary layer [*Guimbaud et al.*, 2002] or for instant, nitric acid can be deposited on ice [*Liao et al.*, 2003]. Also, the heterogeneous reaction of ammonia and nitric acid forming ammonium nitrate can have an important impact on the nitrogen budget.

6. Comparison to Observations

[43] The modeling work so far presented in this paper lined out the special importance of the simulated HNO_3 concentration fields. Therefore some comparison to observations are presented, before the influence of mineral dust on ozone during the MINATROC experiment is discussed.

6.1. Comparison to HNO_3 Observations

[44] Africa is one of the most important regions to study heterogeneous reactions on dust surfaces. The Deposition of Biogeochemically Important Trace Species (DEBITS) program [*Lacaux and Artaxo*, 2003] has established measurement stations in Africa. Nitric acid measurements are published by *Galy-Lacaux et al.* [2001] for the station in Banizoumbou (13.33°N, 2.41°E) located in the Sahelian region of Niger. The region has a dry climate from November to May and a wet season from June to October [*Galy-Lacaux et al.*, 2001]. HNO_3 was measured as monthly integrated samples using passive sampling techniques. We compare the monthly mean measurements to the two model simulations (see Figure 12), but note that the measurements

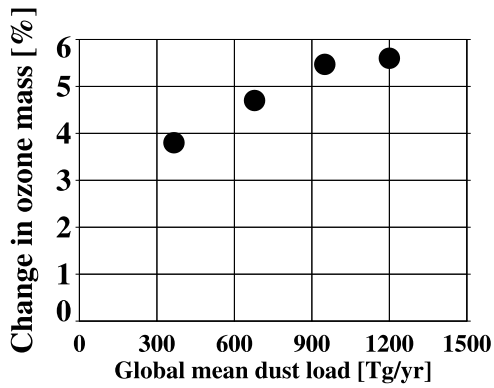

Figure 10. Annual mean changes in ozone mass in percentage for different dust loads.

Table 4. Annual Mean HNO_3 Budget[a]

	CTR	HET
Production		
NO_2 (equation (8))	161	142
NO_3 (equations (9), (10), (12))	1.8	1.6
N_2O_5 (equation (11))	83	78
Total	246	222
Loss		
Dry deposition	91	68
Wet deposition	103	78
Loss on dust		44
Oxidation (equation (14))	30	18
Photolysis (equation (15))	18	11
Total	242	219
Burden, Tg	**3.2**	**2.1**

[a]Units are in Tg (HNO_3) yr^{-1}. CTR, control simulations, where no interaction between mineral aerosols and gas phase species take place; HET, simulation with heterogeneous chemistry.

are taken in 1999 and the model is run under the meteorological conditions of the year 2000. Compared to the observation, the CTR simulation of HNO_3 is highly overestimated. The simulation including the heterogeneous dust reactions, the HET simulation, compares remarkably well to the observations during the seven months of the dry season, which in turn is also the season of frequent dust storms. Heterogeneous chemistry between dust aerosols and nitric acid mainly take place in the dry season. Therefore the two model simulations, HET and CTR, differ mostly during the dry season (see Figure 12). Only during the wet season, from June to October, nitric acid concentrations are still too high in the model. This result is a strong indication that the heterogeneous uptake of nitric acid is well simulated in the model, but that the rain-out processes during the wet season may not be, in this case, efficient enough. (The wet deposition routines of LMDz-INCA are evaluated by *Hauglustaine et al.* [2004].) Nitric acid is highly soluble and thus very efficiently removed in the wet atmosphere. However, this is only a comparison with one measurement station, and so care must be taken in drawing conclusions.

[45] Figure 13 presents a comparison of HNO_3 profiles to several campaign measurements. Even though these campaigns have been carried out during different years, the

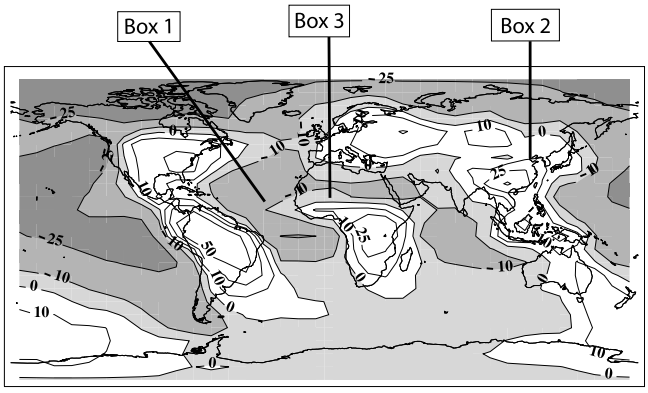

Figure 11. Percentage difference in HNO_3 concentrations between model runs including and excluding thermal decomposition of PAN (%). The three boxes represent the locations for which box model simulations are performed.

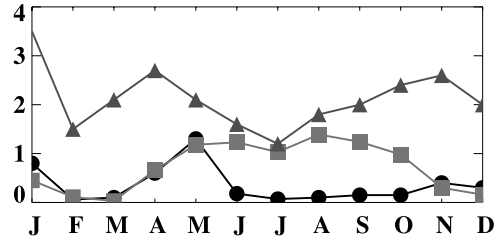

Figure 12. Time series of monthly mean nitric acid mixing ratios ($\mu g\ m^{-3}$) at Banizoumbou in Niger, Africa. Measurements by *Galy-Lacaux et al.* [2001] are marked with black circles; the triangles show results of the CTR simulation, and the squares show results of the HET simulation.

comparison shows clearly that the general overprediction of HNO_3 in models is also present in the CTR simulation. The HET simulation shows significant improvement at nearly all GTE stations, especially in the free troposphere. Nevertheless, HNO_3 still tends to be overestimated. This comparison could be also affected by the large uncertainties linked with nitric acid measurements [see, e.g., *Hanke et al.*, 2003].

6.2. MINATROC Experiment

[46] A suitable location to study the heterogeneous depletion of gaseous species in the presence of mineral dust is the Mount Cimone research station. The station experiences several large dust episodes each year and most episodes occur during summer. The station is situated in the Mediterranean region in northern Italy south of the Alps and the Po valley and north to the Mediterranean Sea at 44°12′N and 10°22′E. Owing to it's altitude, 2165 m above sea level (asl), air sampled at Mount Cimone represents free tropospheric air masses reflecting European continental background conditions. This measurement site is located at about 1600 km from the Saharan desert. The measurement campaign MINATROC took place during 5 weeks in June and July 2000, at Mount Cimone. Subsequently to this extensive field campaign observations of ozone concentration and PM_{10} particle size and mass distribution were carried on until December 2000 by P. Bonasoni et al. (Aerosol and ozone correlation during the dust transport episodes of the summer autumn 2000 period, submitted to *Atmospheric Chemistry and Physics*, 2003, hereinafter referred to as Bonasoni et al., submitted manuscript, 2003). The long-term measurements of coarse aerosol particles, in the size bin of 1–2 μm diameter, is shown in Figure 14. Several dust events can be seen in this time series. During the MINATROC field campaign airborne Saharan dust reached Mount Cimone at the beginning of July. During this event the volume concentration in the measured size bin between 1–2 μm was 3 $\mu m^3\ cm^{-3}$. Stronger dust events were observed during August to October, with maximum volume concentrations exceeding 5 $\mu m^3\ cm^{-3}$. Ten trajectory analysis by Bonasoni et al. (submitted manuscript, 2003) showed that all the measured peaks in coarse aerosol concentrations originate from North Africa. Figure 14 compares the observed aerosol concentrations to the model results. Generally there is a good agreement between the observed most prominent dust events and the model simulation, indicating that the model captures dust uplift in the

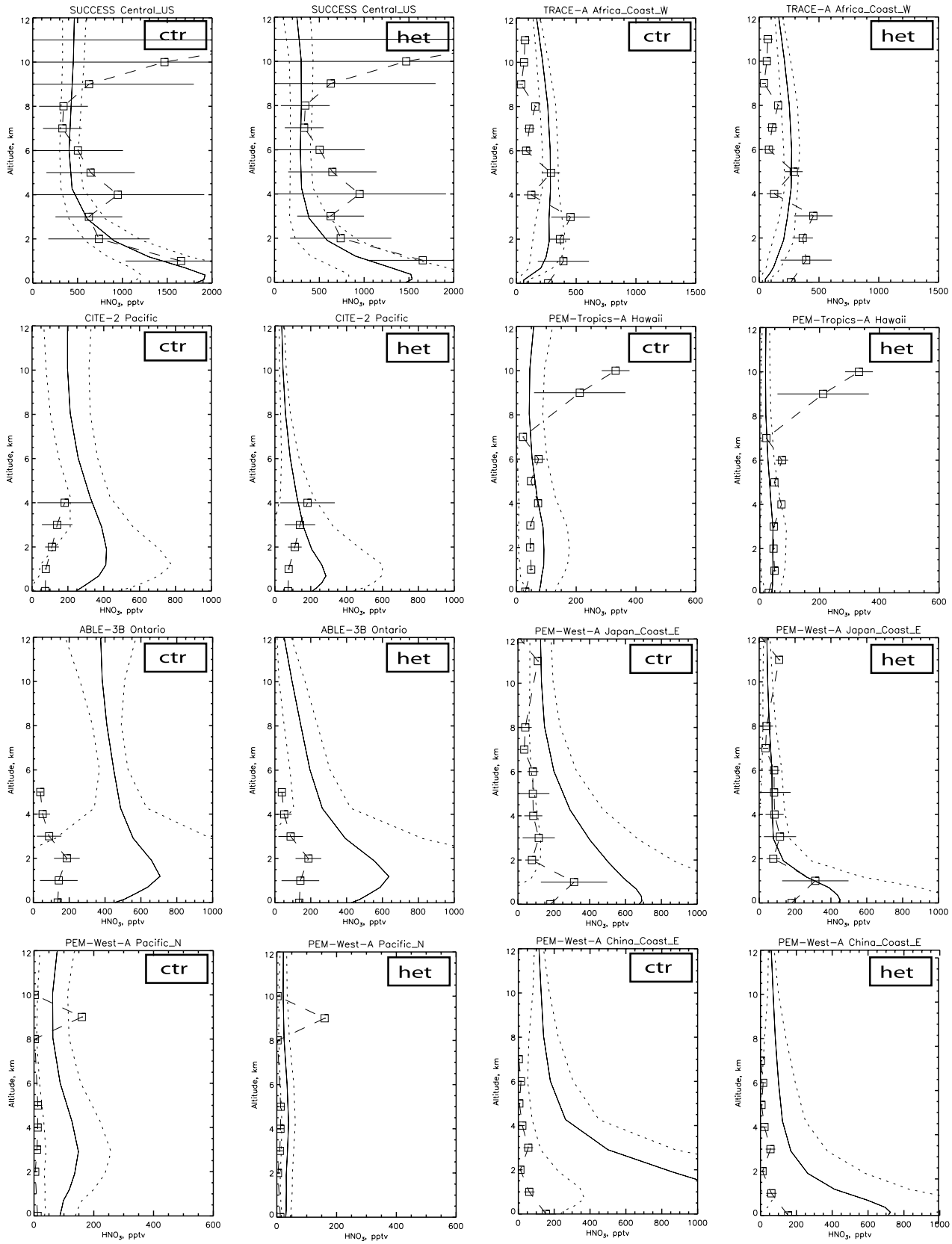

Figure 13. Comparison of observed and simulated (CTR and HET) HNO_3 profiles at the indicated locations. The coordinates for each profile are given by *Emmons et al.* [2000]. The model results are averaged over the given regions and during the duration of the campaigns. Symbols show the observations and the standard deviations. Solid and dotted lines show modeled mean values and standard deviations, respectively.

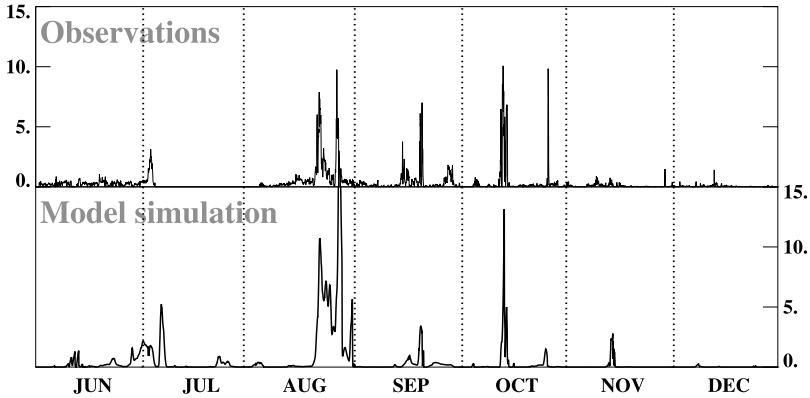

Figure 14. Time series of aerosol volume concentrations (size bin 1–2 μm diameter) at Mount Cimone in μm^3 cm^{-3}. (top) Observations by Bonasoni et al. (submitted manuscript, 2003). (bottom) Model results.

Saharan desert and transport to the Mediterranean region. Furthermore the simulated aerosol volume concentration is comparable to observations.

[47] Intensive measurements were carried out between 1 June and 5 July 2000. Aerosols were observed by means of particle sizing instruments, differential mobility analyzer and optical particle counter [*Putaud et al.*, 2003], LIDAR systems [*Gobbi et al.*, 2003], and impactor measurements. In addition atmospheric trace gases were measured by *Hanke et al.* [2003], Bonasoni et al. (submitted manuscript, 2003), *Fischer et al.* [2002], and other groups participating in the MINATROC campaign [*Balkanski et al.*, 2003a].

[48] During the first weeks of the field campaign no high concentrations of coarse dust particles were measured. The situation changed at the beginning of July. During 3 and 4 July, enhanced coarse aerosol concentrations were observed at the elevation of the station (2165 m asl) [*Putaud et al.*, 2003], and the LIDAR system [*Gobbi et al.*, 2003] observed enhanced aerosol concentrations up to 6 km height. TOMS and SEAWIFS satellite images document that those particles were uplifted in Algeria at 30 June, during a Saharan dust storm and then transported northward over the Mediterranean Sea. After 2–3 days of transport the dust cloud reached Mount Cimone.

[49] This episode is shown in Figure 15. The first panel compares measured and modeled aerosol volume concentrations. The measurements clearly show the low coarse aerosol concentrations before the dust event and the passage of the dust cloud between 2 and 3 July. The analysis of the aerosol chemical composition by *Putaud et al.* [2003] showed that the largest contribution of nitrate was observed in air masses originating from western Europe, whereas the most dominant submicron aerosol mass was made of carbonaceous components in air masses originating from eastern Europe. During the Saharan dust outbreak, Saharan dust and anthropogenic particles seemed to be externally mixed. The measurements show a displacement of NO_3^- toward the aerosol supermicron fraction in presence of dust coarse particles and suggest a significant interaction of HNO_3 with dust particles [*Putaud et al.*, 2003].

[50] The model simulates enhanced aerosol concentrations during the observed dust event (Figure 15), but unfortunately calculates as well enhanced dust concentrations directly before that event. Around 27 June, the model predicts again a small dust event which was not seen by the ground observations, but was observed in higher layers by the LIDAR measurements [see *Gobbi et al.*, 2003, Figure 1]. Even though the simulated aerosol concentrations do not always agree in an absolute sense with to measurements the

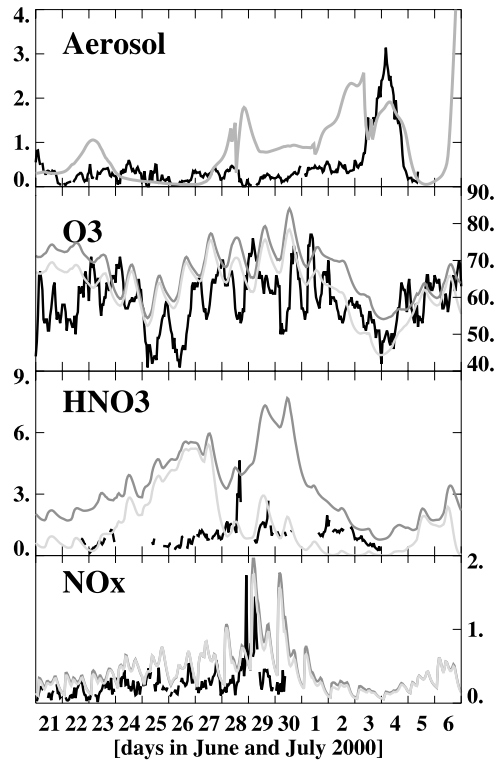

Figure 15. (top) Time series of aerosol volume concentrations (size bin 1–2 μm) at Mount Cimone in μm^3 cm^{-3}. The black line shows observations (Bonasoni et al., submitted manuscript, 2003), and the gray line shows model results. (bottom) Time series of ozone, HNO_3, and NO_x concentrations in ppb_v (observed by Bonasoni et al. (submitted manuscript, 2003), *Hanke et al.* [2003], and *Fischer et al.* [2002], respectively). The black line is observations, the dark gray line is the model CTR simulation, and the light gray line is the HET simulation.

simulated concentration, range of 0–3 μm^3 cm^{-3}, agrees well.

[51] The episode shown in Figure 15, 21 June to 6 July, was influenced during the first days until 23 June, by east European air masses. In the following days the air masses came from western Europe. Polluted air reached the measurement site at the end of June. This event can clearly be seen in the NO_x measurement time series, taken by *Fischer et al.* [2002]. The observations end on 30 June. Both model runs, HET and CTR, don't show large difference in their NO_x simulation, and simulate well the measured concentrations and the arrival of the polluted air masses from western Europe. This pollution event is also clearly visible in the nitric acid measurement [*Hanke et al.*, 2003]. HNO_3 concentrations are lower, between 0.2 to 1.2 ppb_v and increase to 2 ppb_v, before the pollution event. Around 2 July, before the dust event, about 1 ppb_v of nitric acid is measured. During the dust event, HNO_3 is strongly reduced and very low concentrations, even below the detection limit, are measured. The CTR simulation clearly overestimates HNO_3 by a factor of 5 during this event. HNO_3 increases until the end of June, followed by a strong decrease at the beginning of July due to the change in wind direction and the transport of clean Mediterranean air to Mount Cimone. The HET simulation shows much lower nitric acid mixing ratios during the dust event, which is too early in the model. During the dust event the measured and simulated HNO_3 nearly vanish completely, and after the dust cloud has passed the measurement site HNO_3 increases immediately. Both simulated time series show much too high HNO_3 concentrations between 24 and 26 June, too high aerosol concentrations were simulated during the air pollution event, and directly before the dust event. These discrepancies make a comparison difficult. Nevertheless we can conclude that HNO_3 is highly overestimated in the CTR simulation and the HET run is agreeing better with observations. If we consider dust to be present at higher altitudes already on 27 June [see *Gobbi et al.*, 2003] the loss of nitric acid, due to the interaction with dust, might have been visible at higher altitudes.

[52] The ozone measurements (Figure 15, second panel) show high temporal variability, with influence of daily photochemical mixing overlay by large-scale transport processes. Until 24 June east European air transported ozone concentrations up to 70 ppb_v to Mount Cimone. The low concentrations at 25 and 26 June are related to the arrival of Mediterranean air. The highest pollution levels are observed for air masses spending most of their time in the continental boundary layer over NW Europe and arriving at the measurement side between 27 and 30 June 27. The changing wind direction that lead to the transport of clean North African air is clearly visible in the ozone measurements. Ozone decreases by about 20 ppb_v and increases immediately after the dust event. Both simulated time series show the rough temporal evolution during this episode. In the absence of dust, both simulated curves stay close together. During the dust event the model shows in good comparison to the observations a reduced diurnal cycle. The decrease in ozone concentrations during the dust event simulated in the CTR simulation reflects the part in ozone decrease that is related only to transport, because ozone poor air from Africa reaches the measurement side. By contrast, the difference between the HET and the CTR simulation reflect the loss of ozone associated to heterogeneous reactions on the dust aerosols. Following the model results 80% of ozone reduction during this event can be explained by transport and 20% by heterogeneous chemical reactions.

6.3. Continued Observations at Mount Cimone

[53] The dust event which was observed during the MINATROC campaign at Mount Cimone was carrying about 3 μm^3 cm^{-3} aerosol volume concentration in the size bin between 1 and 2 μm at it's maximum intensity, and therefore was monitoring a rather weak dust outbreak. The continued aerosol and ozone measurements by Bonasoni et al. (submitted manuscript, 2003) covered several stronger dust events. Three of those episodes in August, September, and October, respectively are presented in Figure 16.

[54] The dates of the subsequent dust events were perfectly matched by the model. The first dust event in August is associated with a strong decrease in observed ozone concentrations, of about 35 ppb_v. In this case the model simulates that 60% of this decrease is related to transport and 40% to heterogeneous removal processes. At the time of the second event in August no clear signal can be seen in the ozone measurements. In August and the subsequent month the ozone concentration from the two model simulations, CTR and HET, diverge more and more in time, showing the large-scale effect of the heterogeneous chemistry on the background ozone concentration field. Nevertheless the largest differences between the two simulations are still simulated during the dust events. In September and October the simulated dust concentrations compare very well to the measurements. The dust event in October is coincident again with reduced ozone mixing ratios, but in this case the HET simulation underestimates measured ozone concentrations. Table 5 shows the statistical performance of the CTR and the HET simulation of the ozone time series compared to observations on a daily mean basis. The statistical analysis shows that the RMS decreases and the index of agreement increases in the HET simulation, indicating that the simulated ozone concentrations slightly improve in the HET simulation.

7. Summary and Discussion

[55] A global general circulation model, coupled online to atmospheric chemistry and mineral aerosol modules, has been applied to study the impact of heterogeneous chemical reactions at the surface of mineral aerosol on global ozone chemistry. The model simulates Saharan dust well, but probably underestimates dust over eastern Asia and the northern Pacific. Therefore we assume that our estimate gives a lower limit of the heterogeneous loss of ozone precursors in those regions.

[56] We find a global annual mean decrease in tropospheric ozone concentrations of 5% due to heterogeneous chemical reactions. The largest impact is seen over Africa and the equatorial Atlantic where 20% of ozone is lost by reactions on the dust aerosols. The most important reaction pathway for this significant ozone loss is the uptake of gaseous nitric acid on dust aerosols. 35% of nitric acid is removed due to the heterogeneous reactions from the troposphere, leading to a significant loss in the nitrogen

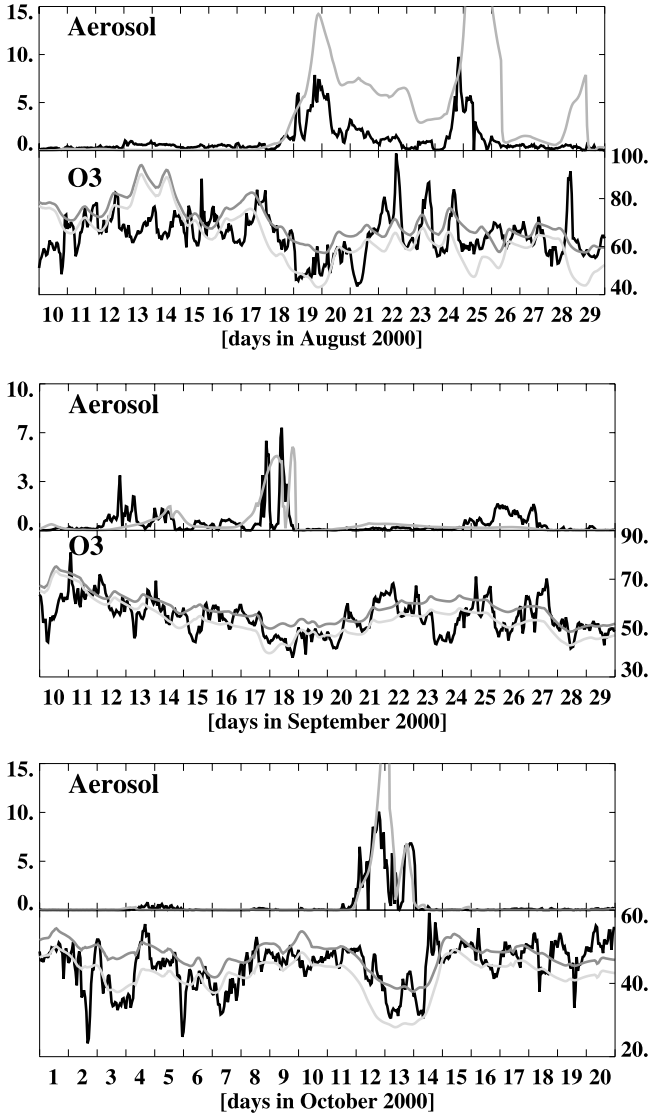

Figure 16. Time series (for August, September, and October 2000) of aerosol volume concentrations (size bin 1–2 μm) and ozone concentrations in ppb_v at Mount Cimone in $\mu m^3\ cm^{-3}$. The black line is observations (Bonasoni et al., submitted manuscript, 2003), the dark gray line is the model CTR simulation, and the light gray line is the HET simulation.

reservoir of the remote atmosphere, and thus reducing ozone production in the clean background atmosphere.

[57] We tested the influence of the uptake process of single chemical species on the global ozone budget and found, that HNO_3 is the most important species in this content. The uptake of just N_2O_5 or NO_3 has a much smaller impact on ozone, less than 1% of tropospheric ozone mass is destroyed via the aerosol uptake of either N_2O_5 or NO_3. The direct uptake of ozone molecules has only a very small impact on the ozone budget. This reaction is only of importance during a dust storm, i.e., in small regions and for limited time periods, and therefore, it appears not to be significant for global modeling.

[58] A major concern in modeling heterogeneous chemical reaction is the uncertainty of the uptake coefficients. This study, in which we tested the range of uncertainty for uptake coefficients of HNO_3, N_2O_5 and O_3, showed that the change in global ozone concentration is rather insensitive to these variations, except when the uptake coefficient for HNO_3 is varied by two orders of magnitude, which reflects the difference in the findings of two different laboratory groups. The model results depend strongly on the amount of simulated nitric acid concentration. Typically atmospheric models tend to overestimate nitric acid [*Thakur et al.*, 1999]. Because of its high solubility and uptake probability, nitric acid is highly linked to aerosol chemistry. Models that only include gas-phase chemistry neglect several important loss processes for nitric acid. Our model does not include all pathways of nitrate aerosol formation, and therefore we might still overestimate HNO_3. Globally, few measurement stations monitor HNO_3. We compared our simulations to HNO_3 measurements in Central Africa where dust impact should be large and to GTE profiles and we found an astonishing good agreement with the observations when heterogeneous reactions are included in the simulation.

[59] The MINATROC campaign at Mount Cimone provided a detailed set of aerosol size and chemical composition measurements as well as measurements of gas-phase species. The dust event observed during that field campaign was a significant, but not a huge event, so the interpretation of the observations are quite difficult. Furthermore, the measurement station is located in northern Italy, and thus is very close to one of the most polluted regions in the world.

[60] The chemical mechanism used in our model neglects nonmethane hydrocarbon chemistry and therefore might be too simple to simulate the complex chemistry taking place in highly polluted air masses. Nevertheless, the simulated ozone concentrations resemble the main characteristics of the measurements. We calculate that 80% of the ozone decrease during the dust event can be explained by the transport of non polluted air masses to the station, and that 20% of the ozone loss is caused by heterogeneous reactions in the dust cloud. A stronger dust event was monitored two months later, in August 2000. In this case, the model calculated 60% of ozone loss due to the transport and 40% caused by the dust aerosols.

Table 5. Statistics of Ozone Time Series for the Time Period June–December 2000[a]

Sampling	*n*	Mean	δ	*b*	*a*	RMS	r^2	*d*
Observations	170	50.3	12.3					
CTR daily mean data	170	50.7	10.2	0.6	20.4	4.4	0.91	0.92
HET daily mean data	170	50.4	12.0	0.8	15.1	3.8	0.98	0.98

[a]The terms *n*, *b*, r^2, and *d* are dimensionless, while the remaining terms have units of ppb_v. *n*, number of measurements or model data included in the analysis; δ, the standard deviations; *b*, slope of the least squares linear regression; *a*, the intercept; *d*, the index of agreement [after *Willmott*, 1981].

[61] In summary, because of the general good agreement with observations we conclude that there may be quite a big influence of mineral dust aerosol on atmospheric chemistry. Also it is a very efficient pathway to irreversibly remove HNO_3 from the atmosphere. Our results could probably be interpreted as being in the upper range of its possible impact. However, we might have neglected some other important uptake mechanisms, such as surface reactions of HO_2 and we certainly underestimated the heterogeneous loss processes on dust in east Asia. Mineral dust seems to be the most important aerosol influencing ozone chemistry, but it is not the only one. Research is ongoing in the field of heterogeneous chemistry. Further measurements especially in Africa and Asia are needed to understand the role of mineral aerosols in atmospheric chemistry. In addition, the investigation of further uptake mechanisms is important. For example, in Central Africa where ozone precursors originate from biomass burning sources the uptake of volatile organic components could be of importance. In this study it turned out that the areas of biomass burning in Central Africa are of high importance for the heterogeneous uptake on desert dust aerosols, implying that biomass burning emissions mix with the dust aerosols. Furthermore not much is known about the chemical products that are formed on the aerosol surfaces and what role they may play in atmospheric chemistry.

[62] **Acknowledgments.** This work was founded by the European Commission (DG XII) as part of the project EVK2-CT-1999-00003 MINATROC. The authors would like to thank Andrzej Klonecki and Marie-Angele Filiberti for assistance with the GCM and Louisa Emmons for use of the GTE data composites. We very gratefully acknowledge the help of Gerd Folberth, who performed the box model experiments mentioned in this paper, for his general help with LMDz-INCA.

References

Balkanski, Y., et al. (2003a), The Mt. Cimone, Italy, free tropospheric campaign: Principal characteristics of the gaseous and aerosol composition from European pollution, Mediterranean influences and during African dust events, *Atmos. Chem. Phys. Discuss.*, *3*, 1753–1776.

Balkanski, Y., M. Schulz, T. Claquin, C. Moulin, and P. Ginoux (2003b), Global emissions of mineral aerosol: Formulation and validation using satellite imagery, in *Emission of Atmospheric Trace Compounds*, edited by C. Granier, P. Artaxo, and C. E. Reeves, Kluwer Acad., Norwell, Mass.

Bian, H., and C. S. Zender (2003), Mineral dust and global tropospheric chemistry: Relative roles of photolysis and heterogeneous uptake, *J. Geophys. Res.*, *108*(D21), 4672, doi:10.1029/2002JD003143.

Chapman, S., and T. G. Cowling (1970), *The Mathematical Theory of Nonuniform Gases*, Cambridge Univ. Press, New York.

Claquin, T., M. Schulz, and Y. J. Balkanski (1999), Modeling the mineralogy of atmospheric dust sources, *J. Geophys. Res.*, *104*, 22,243–22,256.

Davis, E. J. (1983), Transport phenomena with single aerosol particles, *Aerosol Sci. Technol.*, *2*, 121–144.

Dentener, F. J., and P. J. Crutzen (1993), Reaction of N_2O_5 on tropospheric aerosol: Impact on the global distributions of NO_x, O_3, and OH, *J. Geophys. Res.*, *98*, 7149–7162.

Dentener, F. J., G. R. Carmichael, Y. Zhang, J. Lelieveld, and P. J. Crutzen (1996), Role of mineral aerosol as a reactive surface in the global troposphere, *J. Geophys. Res.*, *101*, 22,869–22,889.

de Reus, M., F. Dentener, A. Thomas, S. Borrmann, J. Ström, and J. Lelieveld (2000), Airborne observations of dust aerosol over the North Atlantic Ocean during ACE 2: Indication for heterogeneous ozone destruction, *J. Geophys. Res.*, *105*, 15,263–15,275.

Dickerson, R. R., S. Kondragunta, G. Stechnikov, K. Civerolo, B. G. Doddridge, and B. B. Holben (1997), The impact of aerosols on solar ultraviolet radiation and photochemical smog, *Science*, *278*, 827–830.

Emmons, L. K., D. A. Hauglustaine, J. F. Müller, M. A. Carroll, G. P. Brasseur, D. Brunner, J. Stahelin, V. Thouret, and A. Marenco (2000), Data composites of airborne observations of tropospheric ozone and its precursors, *J. Geophys. Res.*, *105*, 20,497–20,538.

Fischer, H., R. Kormann, T. Klüpfel, C. Gurk, R. Königsted, U. Parchatka, J. Mühle, T. S. Rhee, C. A. M. Brenninkmeijer, P. Bonasoni, and A. Stohl (2002), Ozone production and trace gar correlations during the June 2000 MINATROC intensive measurement campaign at Mt. Cimone, *Atmos. Chem. Phys. Discuss.*, *2*, 1509–1543.

Fuchs, N. A., and A. G. Sutugin (1970), *Highly Dispersed Aerosols*, 105 pp., Butterworth-Heinemann, Woburn, Mass.

Galy-Lacaux, C., G. R. Carmichael, C. H. Song, J. P. Lacaux, H. Al Ourabi, and A. I. Modi (2001), Heterogeneous processes involving nitrogenous compounds and Saharan dust inferred from measurements and model calculations, *J. Geophys. Res.*, *106*, 12,559–12,578.

Gobbi, G. P., F. Barnaba, R. V. Dingenen, J.-P. Putaud, M. Mircea, and M. C. Facchini (2003), Lidar and in situ observations of continental and Saharan aerosol: Closure analysis of particles optical and physical properties, *Atmos. Chem. Phys. Discuss.*, *3*, 445–447.

Goodman, A. L., G. M. Underwood, and V. H. Grassian (2000), A laboratory study of the heterogeneous reaction of nitric acid on calcium carbonate particles, *J. Geophys. Res.*, *105*, 29,053–29,064.

Goudie, A. S. (1983), Dust storms in space and time, *Prog. Phys. Geog.*, *7*, 502–530.

Grassian, V. H. (2001), Heterogeneous uptake and reaction of nitrogen oxides and volatile organic compounds on the surface of atmospheric particles including oxides, carbonates, soot and mineral dust: Implications for the chemical balance of the troposphere, *Int. Rev. Phys. Chem.*, *20*, 467–548.

Guelle, W., Y. J. Balkanski, M. Schulz, F. Dulac, and P. Monfray (1998), Wet deposition in a global size-dependent aerosol transport model: 1. Comparison of a 1 year ^{210}Pb simulation with ground measurements, *J. Geophys. Res.*, *103*, 11,429–11,446.

Guimbaud, C., F. Arens, L. Gutzwiller, H. W. Gäggeler, and M. Ammann (2002), Uptake of HNO_3 to deliquescent sea-salt particles, *Atmos. Phys. Chem.*, *2*, 249–257.

Hanisch, F., and J. N. Crowley (2001), The heterogeneous reactivity of gaseous nitric acid on authentic mineral dust samples, and on individual mineral and clay mineral components, *Phys. Chem. Chem. Phys.*, *3*, 2474–2482.

Hanisch, F., and J. N. Crowley (2003a), Ozone decomposition on Saharan dust: An experimental investigation, *Atmos. Chem. Phys.*, *3*, 119–130.

Hanisch, F., and J. N. Crowley (2003b), Heterogeneous reactivity of NO and HNO_3 on mineral dust in the presence of ozone, *Phys. Chem. Chem. Phys.*, *5*, 883–887.

Hanke, M., B. Umann, J. Uecker, F. Arnold, and H. Bunz (2003), Atmospheric measurements of gas-phase HNO_3 and SO_2 using chemical ionization mass spectrometry during the MINATROC field campaign 2000 on Monte Cimone, *Atmos. Chem. Phys.*, *3*, 417–436.

Hauglustaine, D., F. Hourdin, L. Jourdain, M.-A. Filiberti, S. Walters, and J.-F. Lamarque (2004), Interactive chemistry in the Laboratoire de Météorologie Dynamique general circulation model: Description and background tropospheric chemistry evaluation, *J. Geophys. Res.*, *109*, doi:10.1029/2003JD003957, in press.

He, S., and G. R. Carmichael (1999), Sensitivity of photolysis rates and ozone production in the troposphere to aerosol properties, *J. Geophys. Res.*, *104*, 26,307–26,324.

Herman, J. R., P. K. Bhartia, O. Torres, C. Hsu, C. Seftor, and E. Celarier (1997), Global distributions of UV-absorbing aerosols from Nimbus 7/TOMS data, *J. Geophys. Res.*, *102*, 16,911–16,922.

Hourdin, F., and A. Armengaud (1999), The use of finite-volume methods for atmospheric advection of trace species: Test of various formulations in a general circulation model, *Mon. Weather Rev.*, *127*, 822–837.

Houweling, S., F. Dentener, and J. Lelieveld (1998), The impact of nonmethane compounds on tropospheric photochemistry, *J. Geophys. Res.*, *103*, 10,673–10,696.

Hu, J. H., and J. P. Abbatt (1997), Reaction probabilities for N_2O_5 hydrolysis on sulfuric acid and ammonium sulfate aerosols at room temperatures, *J. Phys. Chem.*, *101*, 871–878.

Husar, R. B., J. M. Prospero, and L. L. Stowe (1997), Characterization of tropospheric aerosols over the oceans with the NOAA advanced very high resolution radiometer optical thickness operational product, *J. Geophys. Res.*, *102*, 16,889–16,909.

Jacob, D. J. (2000), Heterogeneous chemistry and tropospheric ozone, *Atmos. Environ.*, *34*, 2131–2159.

Jacob, D. J., et al. (1996), Origin of ozone and NO_x in the tropical troposphere: A photochemical analysis of aircraft observations over the South Atlantic basin, *J. Geophys. Res.*, *101*, 24,235–24,250.

Jaenicke, R. (1993), Tropospheric aerosols, in *Aerosol-Cloud-Climate Interactions*, edited by P. V. Hobbs, pp. 1–31, Academic, San Diego, Calif.

Jourdain, L., and D. A. Hauglustaine (2001), The global distribution of lightning NO_x simulated on-line in a general circulation model, *Phys. Chem. Earth, Part C*, *26*, 585–591.

Lacaux, J. P., and P. Artaxo (2003), DEPITS: Past, present, and future, *IGAC Newsl.*, *27*, 2–6.

Li, D., and K. P. Shine (1995), A 4-dimensionl ozone climatology for UGAMP models, *Tech. Rep. 35*, U.K. Univ. Global Atmos. Model. Prog., Reading, U. K.

Liao, H., P. J. Adams, S. H. Chung, J. H. Seinfeld, L. J. Mickley, and D. J. Jacob (2003), Interactions between tropopheric chemistry and aerosols in a unified general circulation model, *J. Geophys. Res.*, *108*(D1), 4001, doi:10.1029/2001JD001260.

Lunt, D. J., and P. J. Valdes (2002), The modern dust cycle: Comparison of model results with observations and study of sensitivities, *J. Geophys. Res.*, *107*(D23), 4669, doi:10.1029/2002JD002316.

Martin, R. V., D. J. Jacob, R. M. Yantosca, M. Chin, and P. Ginoux (2003), Global and regional decreases in tropospheric oxidants from photochemical effects of aerosols, *J. Geophys. Res.*, *108*(D3), 4097, doi:10.1029/2002JD002622.

Michel, A. E., C. R. Usher, and V. H. Grassian (2002), Heterogeneous and catalytic uptake of ozone on mineral oxides and dust: A Knudsen cell investigation, *Geophys. Res. Lett.*, *29*(14), 1665, doi:10.1029/2002GL014896.

Michel, A. E., C. R. Usher, and V. H. Grassian (2003), Reactive uptake of ozone on mineral oxides and mineral dust, *Atmos. Environ.*, *37*, 3201–3211.

Ott, S. T., A. Ott, D. W. Martin, and J. A. Young (1991), Analysis of trans-Atlantic Saharan dust outbreak based on satellite and GATE data, *Mon. Weather Rev.*, *119*, 1832–1850.

Phadnis, M. J., and G. R. Carmichael (2000), Numerical investigation of the influence of mineral dust on tropospheric chemistry of East Asia, *J. Atmos. Chem.*, *36*, 285–323.

Prospero, J. M. (1995), The atmospheric transport of particles to the ocean, in *Particle Flux into the Ocean*, *SCOPE Rep. 57*, edited by V. Ittekkot, S. Honjo, and P. J. Depertris, pp. 19–52, John Wiley, Hoboken, N. J.

Prospero, J. M., P. Ginoux, O. Torres, S. Nicholson, and T. E. Gill (2002), Environmental characterization of global sources of atmospheric soil dust identified with the Nimbus 7 Total Ozone Mapping Spectrometer (TOMS) absorbing aerosol product, *Rev. Geophys.*, *40*(1), 1002, doi:10.1029/2000RG000095.

Putaud, J.-P., R. V. Dingenen, A. Dell'Acqua, F. Raes, E. Matta, S. Decesari, M. C. Facchini, and S. Fuzzi (2003), Size-segregated aerosol mass closure and chemical composition in Monte Cimone (I) during MINATROC, *Atmos. Chem. Phys. Discuss.*, *3*, 4097–4127.

Ravishankara, A. R. (1997), Heterogeneous and multiphase chemistry in the troposphere, *Science*, *276*, 1058–1065.

Rudich, Y., R. K. Talukdar, A. R. Ravishankara, and R. W. Fox (1996), Reactive uptake of NO_3 on pure water and ionic solutions, *J. Geophys. Res.*, *101*, 21,023–21,031.

Sadourny, R., and K. Laval (1984), January and July performance of the LMD general circulation model, *New Perspectives in Climate Modeling*, vol. 1, edited by A. Berger and C. Nicolis, pp. 173–197, Elsevier Sci., New York.

Saylor, R. D. (1997), An estimate of the potential significance of the heterogeneous loss to aerosols as an additional sink for hydroperoxyd radicals in the troposphere, *Atmos. Environ.*, *31*, 3653–3658.

Schulz, M., Y. J. Balkanski, W. Guelle, and F. Dulac (1998), Role of aerosol size distribution and source location in a three-dimensional simulation of a Saharan dust episode tested against satellite-derived optical thickness, *J. Geophys. Res.*, *103*, 10,579–10,592.

Tegen, I., and R. Miller (1998), A general circulation model study on the interannual variability of soil dust aerosol, *J. Geophys. Res.*, *103*, 25,975–25,995.

Tegen, I., S. P. Harrison, K. Kohfeld, I. C. Prentice, M. Coe, and M. Heimann (2002), Impact of vegetation and preferential source areas on global dust aerosol: Results from a model study, *J. Geophys. Res.*, *107*(D21), 4576, doi:10.1029/2001JD000963.

Thakur, A. N., H. B. Singh, P. Mariani, Y. Chen, Y. Wang, D. J. Jacob, G. Brasseur, J. F. Müller, and M. Lawrence (1999), Distribution of reactive nitrogen species in the remote free troposphere: Data and model comparison, *Atmos. Environ.*, *33*, 1403–1422.

Thomas, K., A. Volz-Thomas, D. Mihelcic, H. G. J. Smit, and D. Kley (1998), On the exchange of NO_3 radicals with aqueous solutions: Solubility and sticking coefficient, *J. Atmos. Chem.*, *29*, 17–43.

Tiedtke, M. (1989), A comprehensive mass flux scheme for cumulus parameterization in large-scale models, *Mon. Weather Rev.*, *117*, 1779–1800.

Underwood, G. M., C. H. Song, M. Phadnis, G. R. Carmichael, and V. H. Grassian (2001), Heterogeneous reactions of NO_2 and HNO_3 on oxides and mineral dust: A combined laboratory and modeling study, *J. Geophys. Res.*, *106*, 18,055–18,066.

van Leer, B. (1977), Towards the ultimate conservative difference scheme. part IV: A new approach to numerical convection, *J. Comput. Phys.*, *23*, 276–299.

Willmott, C. J. (1981), On the validation of models, *Phys. Geogr.*, *2*, 168–194.

Woodward, S. (2001), Modeling the atmospheric life cycle and radiative impact of mineral dust in the Hadley Centre climate model, *J. Geophys. Res.*, *106*, 18,155–18,166.

Zender, C. S., H. Bian, and D. Newman (2003), Mineral dust entrainment and deposition (DEAD) model: Description and 1990s dust climatology, *J. Geophys. Res.*, *108*(D14), 4416, doi:10.1029/2002JD002775.

Zhang, Y., Y. Sunwoo, V. Kotamarthi, and G. R. Carmichael (1994), Photochemical oxidant processes in the presence of dust: An evaluation of the impact of dust on particulate nitrate and ozone formation, *J. Appl. Meteorol.*, *33*, 813–824.

Y. Balkanski, D. A. Hauglustaine, and M. Schulz, Laboratoire des Sciences du Climat et de l'Environnement, Centre National de la Recherche Scientifique/Commissariat à l'Energie Atomique, L'Orme des Merisiers, F-91191 Gif-sur Yvette, France. (balkanski@cea.fr; hauglustaine@cea.fr; schulz@cea.fr)

S. E. Bauer, NASA Goddard Institute for Space Studies, The Earth Institute at Columbia University, 2880 Broadway, New York, NY 10025, USA. (sbauer@giss.nasa.gov)

F. Dentener, Joint Research Center, Institute for Environment and Substainability, Building 29, Via Enrico Fermi, I-21020 Ispra (VA), Italy. (frank.dentener@jrc.it)